Available online at www.sciencedirect.com
SCIENCE DIRECT®
Talanta 60 (2003) 303–312
Talanta
www.elsevier.com/locate/talanta

A new method for immunoassays using field-flow fractionation with on-line, continuous chemiluminescence detection☆

D. Melucci [a], M. Guardigli [b], B. Roda [a], A. Zattoni [a], P. Reschiglian [a], A. Roda [b,*]

[a] Department of Chemistry 'G. Ciamician', Via Selmi 2, 40126 Bologna, Italy
[b] Department of Pharmaceutical Sciences, Via Belmeloro 6, 40126 Bologna, Italy

Received 23 July 2002; received in revised form 9 October 2002; accepted 10 October 2002

Abstract

Chemiluminescence detection has already been combined with different separation techniques such as HPLC and capillary electrophoresis. In this work, it was applied to gravitational field-flow fractionation, a low-cost, flow-assisted separation technique for micronsized particles suited to further on-line detection of the separated analytes. Horseradish peroxidase was used as model sample, either free in solution or immobilized onto micronsized, polystyrene beads. The chemiluminescent substrates were added directly into the mobile phase, and the continuous, steady-state chemiluminescence generated during elution was detected on-line by either a flow-through luminometer or a CCD camera. Ultra-low detection limits, two orders of magnitude lower than those achievable with spectrophotometric detection, were found. The possibility to fully separate and quantitate free and bead-immobilized enzymes is reported, as a step towards the development of multianalyte, ultra-sensitive, micronsized beads-based flow-assisted immunoassays.

Keywords: Chemiluminescence; Field-flow fractionation; Imaging; Immunoassays

1. Introduction

Chemiluminescence (CL) detection has been successfully applied to several flow-through analytical techniques, including flow injection analysis (FIA), separation methods such as pre- and post-column HPLC [1] and capillary electrophoresis (CE) [2]. With these techniques, CL detection potentially enhances signal detectability and selectivity with respect to conventional UV/Visible (UV/Vis) spectrophotometric and fluorescence detection. This can be achieved because the emitted light is actually generated in the dark as a result of a specific chemical reaction, which is often catalysed by an enzyme [3]. CL-based methods offer many advantages with respect to UV/Vis spectrophotometric methods [4], and they find extensive application, particularly in bioanalytical chemistry [5,6]. Various, reliable CL sys-

☆ Work presented at: X International Symposium on Luminescence Spectrometry-Detection Techniques in Flowing Streams—Quality Assurance and Applied Analysis (ISLS 2002), 4–7 June, 2002, Granada, Spain.

* Corresponding author. Tel./fax: +39-051-343-398.
E-mail address: roda@alma.unibo.it (A. Roda).

0039-9140/03/$ - see front matter
doi:10.1016/S0039-9140(03)00106-1

tems for the ultrasensitive detection (down to zeptomole levels) of enzymes such as horseradish peroxidase (HRP), alkaline phosphatase, and β-galactosidase have been developed [7]. In most cases the CL emission kinetics is very fast and once the CL reaction has occurred, steady-state light intensity is obtained after a few seconds. Under optimised conditions and in excess of the CL substrate, the steady-state CL intensity is proportional to the enzyme activity, which allows for easy quantitative analysis. Not only enzymes or enzyme-labelled biospecific probes (e.g. antibodies, nucleic acids) can be detected by CL, but also direct CL, flash-type reactions can be employed, once the procedure has been standardized [8]. Although CL detection is highly selective, separation of the analytes before detection may still be required, as in heterogeneous immunoassays. It is noteworthy that protein complexes, nucleic acids, enzyme-labelled bio-specific probes, when bound to nano- or micronsized beads for heterogeneous immunoassays cannot be separated by HPLC or CE.

Field-flow fractionation (FFF) is a family of chromatographic-like techniques in which separation is performed, rather than by the interaction with a stationary phase, through an external field that is applied perpendicularly to the mobile phase flow [9]. The application niche of FFF spans macromolecules, nano- and micronsized particulate matter of any origin. High molecular weight proteins, protein complexes, but also nano- and micronsized particles as viruses, bacteria and cells are, for instance, among the dispersed samples of biological origin which have been separated by FFF. FFF can thus play the role of an ideal flow-assisted separation method for many bioanalytical applications. For instance, immunological methods can take advantage of FFF to separate, on a size basis, mixtures of biological macromolecules bound to nano- or micronsized beads, with relatively low cost and short analysis time.

In FFF, sample detection is mostly performed by spectroscopic methods, among which UV/Vis spectrophotometry still constitutes the workhorse. It is known, however, that the main problem of UV/Vis spectroscopic methods in FFF lies in the complex dependence of the detector's response on sample features [10]. UV/Vis spectrophotometric detection is also characterized by lack of specificity and low sensitivity. Fluorescence detection could be applied, although the non specific signal from the sample matrix or reagents can strongly reduce detection performance [11,12]. Either in spectrophotometric or fluorescence detection, interaction of the incident radiation with the sample is complex because of the heterogeneous nature of the sample/dispersing medium system. Flow cytometry (FC) can effectively exploit the analytical response from the UV/Vis light source on the dispersed, sorted particles, and FC has been applied successfully to FFF of biological, micronsized samples like cells [13,14]. However, FC is an expensive technique and it is not enough sensitive for quantitative analysis at trace levels. For all the above evidences, UV/Vis methods are lacking for the analysis and characterization of biological species in dispersed forms. Otherwise, the above limitations could be overcome using ultrasensitive detection methods based on the measurement of the photons that are directly generated by the sample itself without incident radiation, such as CL. Very recently a FFF–FIA–CL system based on post-column CL detection was described [15,16].

In this work, FFF coupled with continuous, on-line CL detection is for the first time presented for the development of ultrasensitive, highly-selective, micronsized beads-based flow-assisted immunoassays. HRP, free or immobilized onto micronsized polystyrene (PS) beads, was used as the model analyte. The CL-inducing cocktail (luminol/H_2O_2/*p*-iodophenol) was directly added to the mobile phase. HRP catalyses the CL reaction and gives a continuous CL signal sufficiently stable during the complete FFF run. By this way, post-column reactions are not required. Gravitational FFF (GrFFF), the simple, low-cost subset of sedimentation FFF that uses Earth's gravitational field to achieve separation, was employed. This is because of two reasons. First, GrFFF was successfully applied to a wealth of micronsized, dispersed samples of either inorganic [17,18] or biological origin [19]. The GrFFF elution mode of such samples is defined as steric/hyperlayer or focusing mode. In steric/hyperlayer GrFFF hydrodynamic

effects, such as lift forces, counteract the primary field generated by the Earth's gravitational field and tend to make sample particles form a narrow band (hyperlayer) at some distance from the accumulation wall. Analytes in steric/hyperlayer GrFFF are then separated not only on a size and density basis but also on a complex combination of different morphological and surface features on which lift forces are known to depend [20]. This aspect makes GrFFF particularly exploitable for the characterization of micronsized particles of biological origin. Second, the chemical inertness of the GrFFF channel avoids possible interference with the CL reaction (e.g. quenching or aspecific CL signal). We demonstrate that GrFFF–CL, when compared to UV/Vis spectrophotometric detection, produces approximately a 100-fold reduction in the limit of detection of enzymes linked to micronsized beads. On-line, continuous GrFFF–CL coupling also displays the key feature of being able to perform efficient separation and quantification of free and bound HRP. It might be thus developed for fast immunoassays based on the separation of bead-bound antibodies.

2. Materials and methods

Samples were surface-carboxylated PS beads 6.10 ± 0.57 or 3.00 ± 0.14 μm in diameter (Polysciences Inc., Warrington, PA) coated with HRP (EC 1.11.1.7, type VI-A, from Sigma Chemical Co, St. Louis, MO), hereafter indicated as PS/HRP 6 μm and PS/HRP 3 μm, respectively. HRP was immobilized on the PS beads following the protocol reported by the manufacturer for covalent bonding of proteins (Polysciences Inc., Technical Data Sheet 238C). The method involves the formation of an amide bond with the primary lysine amine residues of the enzyme, and employs water-soluble 1-(3-dimethylaminopropyl)-3-ethyl carbodiimide hydrochloride (EDAC, from Sigma) for the activation of the carboxyl groups on the PS bead surface.

The GrFFF channel was home-built as described elsewhere [20]. The depletion wall was made of polycarbonate and the accumulation wall of polyvinyl chloride. Both walls were transparent, thus allowing the CL signal to be measured within the channel. Nominal channel dimensions were 30.0 cm tip-to-tip in length, 2.0 cm in breadth, and 0.0140 cm in thickness, giving a nominal channel surface of 55.0 cm^2 and a nominal channel volume of 0.77 ml. The channel simply replaced the column in a HPLC system. The carrier flow was delivered by an HPLC pump, model 9010 (Varian, Walnut Creek, CA). The injection port was a Rheodyne loop valve model 7125 equipped with a 5-μl loop. Samples were injected at a flow rate of 0.2 ml min^{-1} for 15 s. Before the elution the flow was stopped for 5 min (PS/HRP 6 μm) or 15 min (PS/HRP 3 μm) to allow particles to relax and reach their equilibrium position inside the channel. The mobile phase employed for GrFFF of PS particles (TRIS buffer 0.01 M, pH 8.6, containing SDS 0.05% w/v) was modified by adding hydrogen peroxide (30 ppm) and luminol (1 mM) to induce continuous CL due to the HRP-catalysed oxidation of luminol. An enhancer (*p*-iodophenol 10 μM) was also added to increase the intensity and stability of the CL signal. Imaging of the CL signal from the PS/HRP 6 μm beads before the injection was obtained by resuspending the particles in the mobile phase added with the CL cocktail, and observing them through an Olympus BX-40 epifluorescence microscope (Olympus, Tokyo, Japan) coupled with a liquid nitrogen-cooled CCD camera (Model LN/CCD Princeton Instruments, Roper Scientific, Trenton, NJ). The CL signal was then acquired and processed using image processing software (Metamorph v. 4.5, Universal Imaging Corporation, West Chester, PA).

Two FFF-CL systems were employed in this work. In the first system, hereafter indicated as GrFFF–CL, the GrFFF channel outlet was fed to a HPLC UV/Vis detector model 2550 (Varian) operating at 400 nm, and the outlet of the UV/Vis detector cell was fed to a photomultiplier-based flow-cell luminometer (Lumiflow, Immunotek, Moscow, Russia) whose original flow-through cell was home-modified to improve detection sensitivity by increasing the cell volume to about 20 μl. The turbidimetric signal from the UV/Vis detector was captured using a 12-bit I/O DAQ board, model 6040E (National Instruments, Aus-

tin, TX), plugged into a PC Pentium III 350 MHz and driven by LabView® 5.0 (National Instruments) home-built software. The luminometer was connected to a Pentium III 350 MHz PC through the RS-232 port, and the CL signal was recorded using the data acquisition software provided by the manufacturer (Flowreg Data Registration software v. 1.0, Immunotek) to obtain the flow-through CL fractograms. To allow for direct comparison between the analytical performance of UV/Vis and CL detection, both the signals were acquired with the same sampling interval (1 s). Due to the complex nature of the FFF noise [21], the limit of detection (LoD) values were evaluated from the signal-to-noise ratio of the fractograms. Noise standard deviation was determined by transforming the sample band of the fractogram into a frequency domain by fast Fourier transform algorithms implemented in PeakFit v.4 (SPSS Science, Chicago, IL). Fourier transform was applied on those data points flanking the sample band maximum by less than $\pm$5-fold the band half-width. The frequency spectrum was filtered by applying a low-pass filtering function whose frequency cut-off was determined in order to isolate the noise frequency components from the signal component [22]. The filtered noise in the time domain was afterward restored by a backward Fourier transform. The LoD was thus determined as the amount of injected sample giving a peak height equal to three times the noise standard deviation.

In the second system, hereafter indicated as GrFFF–CL/CCD, the continuous CL emission was measured from the channel during the elution of the samples by using a low-light luminograph (Night Owl LB 981, EG&G Berthold, Bad Wildbad, Germany) equipped with a highly sensitive, back-illuminated, Peltier-cooled CCD camera. The sample chamber of the luminograph was large enough to contain both the GrFFF channel and the Rheodyne valve, while the HPLC pump was outside of the instrument. Images of the CL signal from the GrFFF channel were acquired at 15-s intervals during elution, using an exposure time of 5 s. The images were then analysed using MatLab 6.0 (The MathWorks, Natick, MA). Each CL image was corrected for the background signal, then the profiles of the CL intensity versus the adimensional channel length (z) were obtained by integration of the CL signal along the channel width. These resulting profiles are hereafter called bands in the length coordinate (z-bands). The CL signals were also integrated over a rectangular window at the outlet of the channel to obtain the profiles of the CL signal as a function of time (hereafter called bands in the time coordinate, t-bands). These profiles virtually are flow-through CL fractograms obtained by in-channel detection.

3. Results and discussion

3.1. PS/HRP: immobilization efficiency

It is known that immobilisation efficiency is a critical factor that affects the performance of immunoassays based on immobilised biospecific reagents. For the PS/HRP model sample, the immobilization efficiency can be evaluated by comparing the CL signals from PS/HRP samples to those given by free HRP. However, it must be taken into account that the immobilisation of enzymes usually modifies the enzyme activity. The theoretical maximum number of HRP molecules bound to a PS bead can be calculated assuming a monolayer cubic close packing of HRP on the PS bead surface. The 'monolayer coating' assumption is reasonable since the formation of a multilayer enzyme coating may take place, in fact, as a consequence of protein cross-linking. This requires the activation of the carboxyl groups of the enzyme. In fact, in the coating procedure here employed, only the carboxyl groups on the PS bead surface are activated, hence protein cross-linking might not be possible. For example, in the case of PS/HRP 6 μm, if one takes from the literature the spherical molecular diameter of the HRP molecule (4.6 nm) [23], one can get a theoretical maximum value of 5.3×10^6 HRP molecules per PS bead, corresponding to a bound HRP/PS bead mass ratio of about 1/300. On the other hand, the ratio between the slopes of the calibration curves obtained by integrating the CL-fractogram peaks for bound and free HRP (see Section 3.3) resulted to be 1/350. Reasonable

agreement between these mass ratio values supports the assumption of a complete, monolayer coating of HRP molecules on PS beads. On the other hand, it also indicates that the activity of HRP is here just slightly affected by its immobilization.

3.2. UV/Vis versus CL

Fig. 1a and 1b show the fractograms obtained in the GrFFF–CL system for the injection of 10 μg of PS/HRP 6 μm and PS/HRP 3 μm, respectively. Superimposition of GrFFF–CL fractograms obtained from repeated runs indicates excellent inter-run reproducibility. The flow-through CL fractograms relevant to the PS/HRP 6 μm and PS/HRP 3 μm show significantly different band shapes, the band of the PS/HRP 6 μm sample being slightly distorted. A large contribution to band distortion in FFF is due to the intrinsic polydispersity of the samples [24]. However, in this case it cannot be excluded that part of the band distortion is an artifact due to the on-line, continuous CL detection, because the excited, CL emitting species are actually formed in solution as a consequence of the reaction catalysed by the bound HRP (see Fig. 2a). Localization of the CL signal close to the PS-bead surface occurs if kinetics of the CL reaction steps are fast compared to the diffusion rates of the reaction intermediates. Direct microscopic observation of the CL signal from the HRP-coated beads (Fig. 2c) shows that the signal is localized in the thin solution layer around the beads, suggesting that diffusion of the excited emitting species can be neglected. Moreover, Fig. 1a and 1b indicate that the peak widths of UV/Vis and CL fractograms are not significantly different and the peak maxima coincide. These findings provide indirect proof that band distortion in this GrFFF–CL system was due to the intrinsic polydispersity of the PS beads, as it is generally the case in FFF, rather than to artifacts related to the on-line, continuous CL detection method. The lower band distortion in the CL fractogram of PS/HRP 3 μm when compared to PS/HRP 6 μm is indeed consistent with the narrower size distribution of PS/HRP 3 μm (3.00 ± 0.14 vs. 6.10 ± 0.57 μm).

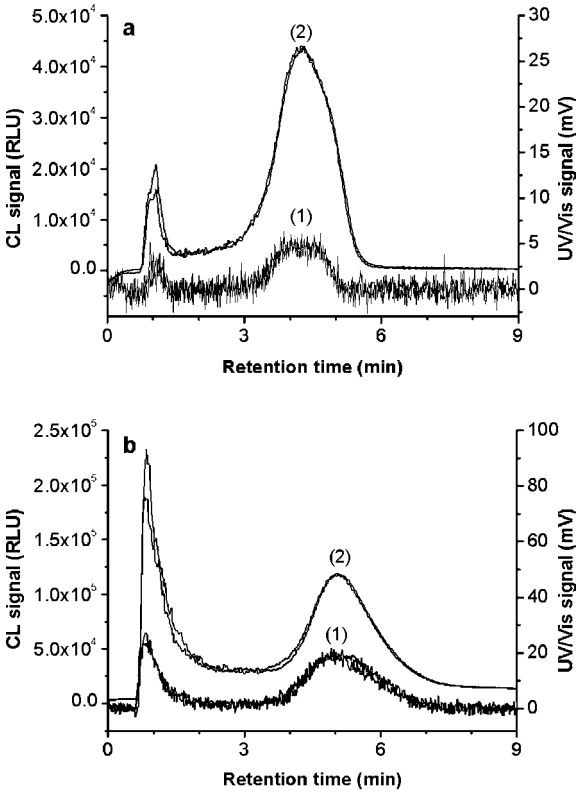

Fig. 1. UV/Vis (1) vs. CL (2) fractograms in GrFFF–CL for the injection of 10 μg of (a) PS/HRP 6 μm and (b) PS/HRP 3 μm. Two repeated runs are superimposed to show inter-run reproducibility. Elution flow rate: 0.75 ml min^{-1}.

3.3. Quantitative analysis

Comparison between area values of sample bands in the CL fractograms and relevant injected masses showed that, in the GrFFF–CL system, the CL responses were linear for both free and bound HRP. Linear regression analysis gave $A = (-0.7 \pm 1.6)10^4 + (1.49 \pm 0.06)10^5 m$ ($R^2 = 0.995$, $N = 9$) and $A = (4.0 \pm 1.1)10^5 + (4.2 \pm 0.2)10^5 m$ ($R^2 = 0.988$, $N = 11$), respectively, for free and bound HRP, where A (min) is the peak area and m the injected sample mass expressed in ng (free HRP) or μg (bound HRP). This finding enables GrFFF–CL for not only reliable separation but also fast, quantitative evaluation of free and bead-bound HRP.

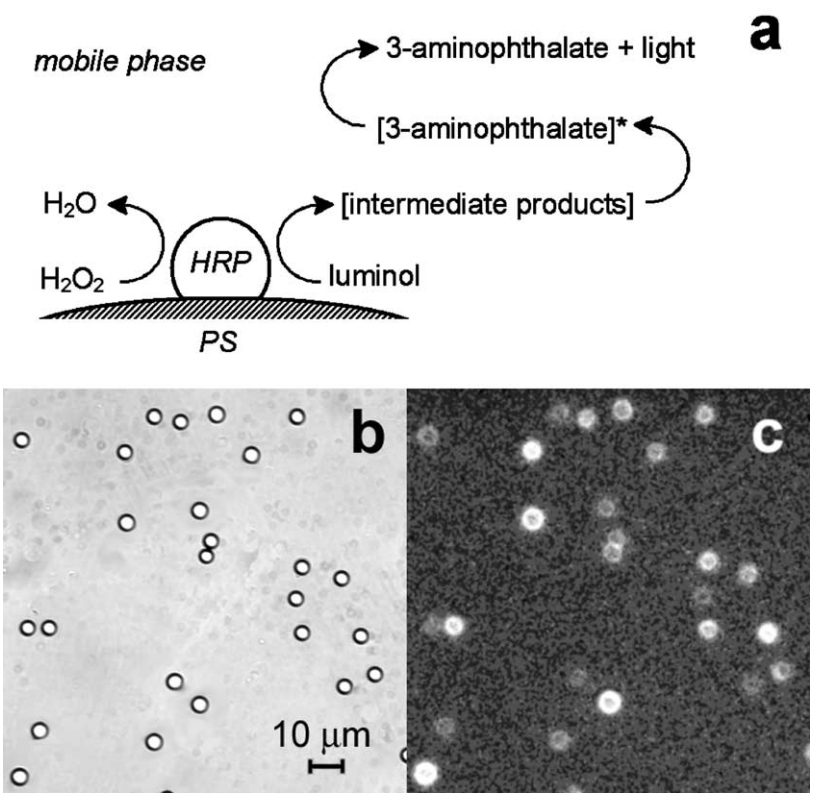

Fig. 2. Schematic representation of the processes leading to CL emission from PS-bound HRP (a), and comparison between the visible light image (b) and the CL signal (c) for a PS/HRP 6 μm sample.

Fig. 3 shows the LoD values obtained from UV/Vis and CL fractograms of PS/HRP 6 μm in the GrFFF–CL system as a function of the injected PS masses. These LoD values were evaluated from the signal-to-noise ratio of the fractograms, determined by Fourier transforms, as described in Section 2. If compared to UV/Vis detection, a reduction of two orders of magnitude in the LoD values for CL is observed. The lowest LoD value in GrFFF–CL, expressed in mass of PS beads, was found to be about 10 ng. This corresponds to a minimum detectable amount of HRP bound to PS of the order of 30 pg (i.e. about 0.7 fmol), with the mass ratio between the immobilized HRP and the supporting PS beads estimated upon the assumptions above discussed in Section 3.1.

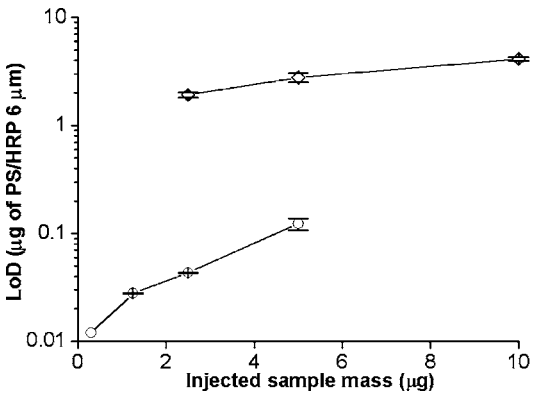

Fig. 3. Limit of detection values for GrFFF–CL of PS/HRP 6 μm as a function of the injected mass. Comparison between UV/Vis (◇) and CL (○) detection.

As far as GrFFF–CL/CCD system is concerned, its goal can be the optimisation of the fractionation process. GrFFF–CL/CCD image analysis can give indications on the ideality of the fractionation mechanism, and handy evaluation of sample recovery. This information cannot

be easily obtained in GrFFF–CL. Otherwise, once the fractionation process has been optimised in GrFFF–CL/CCD, analytical applications can be performed in GrFFF–CL, which is characterized by higher sensitivity and simpler data handling. In Fig. 4 it is reported an example of separation between free (HRP) and bound (PS/HRP 6 μm) enzyme. In the lower-left panel it is shown the CCD image of the real separation of free and bound HRP as it occurs along the channel. In the upper-left panel are reported the relevant CL signal profiles (i.e. the z-bands). In the right panel of Fig. 4 are reported the CL signals of free and bound HRP at the channel end (i.e. the t-bands) once they have been reconstructed by integration within the window indicated in the lower-left panel of the same Figure.

The LoD for the GrFFF–CL/CCD system was calculated from the signal-to-noise ratio of the z-bands. Fig. 5a and b report the LoD values obtained for PS/HRP 6 μm and free HRP (which is eluted with the void time), respectively. Sample bands centred at about $z = 0.5$ and whose profiles showed a return to the baseline at $z = 1$, were used for such a determination. Comparison between Figs. 3 and 5a shows that the LoD value obtained in GrFFF–CL/CCD is significantly higher than in GrFFF–CL. However, it must be pointed out that the noise standard deviations in the z-bands were found to be almost constant, and independent of the nature and amount of the injected sample (PS/HRP 6 μm or free HRP). This clearly indicates that the instrumental noise was the most dominant

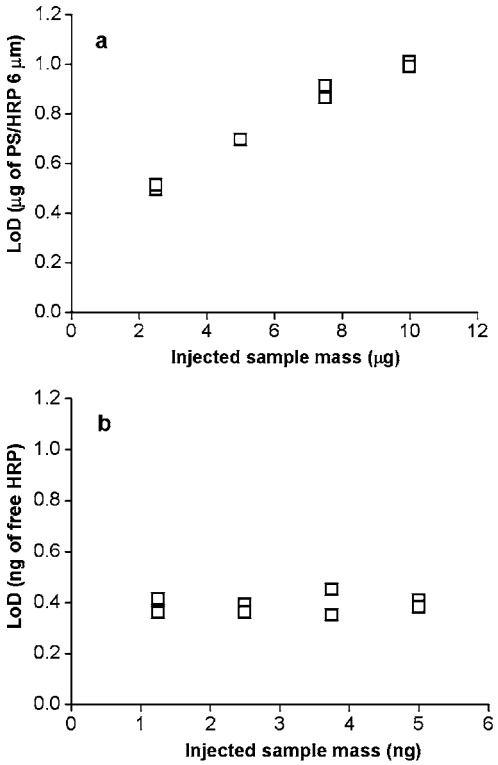

Fig. 5. Limits of detection (LoD) values in GrFFF–CL/CCD from the signal-to-noise ratio values of the z-bands, expressed as a function of the injected mass. (a) PS/HRP 6 μm, (b) free HRP. Elution flow rate: 0.4 ml min^{-1}.

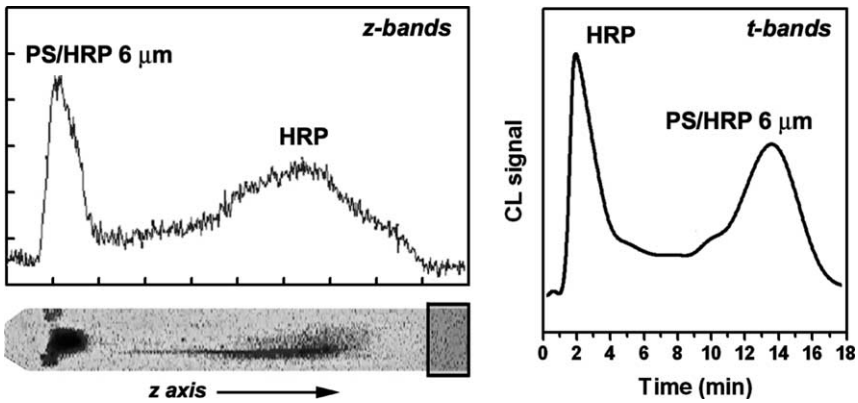

Fig. 4. GrFFF–CL/CCD of a mixture of PS-bound HRP (PS/HRP 6 μm) and free HRP (HRP). Lower-left panel: imaging of the GrFFF channel during separation of PS-bound and free HRP; upper-left panel: CL signal profiles (z-bands) within the GrFFF channel; right panel: reconstructed CL signal at the channel outlet (t-bands).

type of noise in these measurements. LoD values might thus be reduced by decreasing such a noise level. For example, the signal-to-noise ratio could be improved by increasing the exposure time, that is the time used for image acquisition [25]. Fig. 5a,b show that the LoD for PS/HRP 6 μm decreases with decreasing the injected sample mass, as above reported in GrFFF–CL, while the LoD values for HRP is almost constant (about 0.4 ng). It is known that particulate samples retained in GrFFF may suffer of sample overloading, which can affect peak retention parameters [26]. Since unretained analytes are swept down the channel with a homogeneous distribution across the channel thickness, overloading may not affect unretained bands to a significant extent. This fact could explain the observed independence of the HRP LoD values of the HRP injected mass. At the lowest injected masses, the LoD for PS/HRP 6 μm tends to a value of about 300 ng. Assuming that the mass ratio between the bound HRP and the supporting PS bead corresponds to ca. 1/300, as above reported in Section 3.1, then the LoD of PS/HRP 6 μm would correspond to about 1 ng of bound HRP, which is rather close value to the LoD value found for free HRP. This finding eventually supports the estimated amount, and relevant activity, of PS-bound HRP above discussed in Section 3.1.

The possibility to separate and quantify mixtures of free and bound enzyme was further tested in GrFFF–CL/CCD. Fig. 6 reports the *t*-bands obtained from mixtures of free HRP and PS/HRP 6 μm, which demonstrate that no unrelaxed particles elute with the void time. This is a key requirement for the development of immunoassays based on the separation of free and bead-bound analytes. Preliminary experiments (data not reported) in GrFFF–CL/CCD again showed good correlation between the band areas and the amounts of free and bound HRP in the injected samples, as already found in GrFFF–CL, confirming that simultaneous quantification of the separate components is also possible in GrFFF–CL/CCD. CCD image analysis of the channel after each separation run always gave also direct indication that neither free enzyme (HRP) nor bound enzyme (PS/HRP) was trapped at amounts above the LoD in GrFFF–CL/CCD. Although a systematic study on sample recovery is beyond the aims of the present paper, the absence of sample trapping inside the channel also represents a key point as far as FFF-based immunoassay development is concerned.

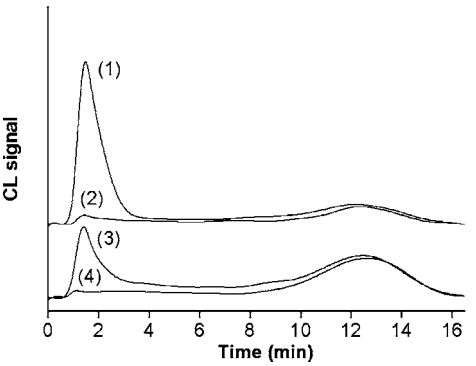

Fig. 6. Comparison between *t*-bands obtained in GrFFF–CL/CCD from the injection of mixtures of free HRP and PS/HRP 6 μm. Injected masses: (1) 3.75 ng free HRP and 2.5 μg PS/HRP 6 μm; (2) 2.5 μg PS/HRP 6 μm; (3) 1.25 ng free HRP and 7.5 μg PS/HRP 6 μm; (4) 7.5 μg PS/HRP 6 μm. Elution flow rate: 0.4 ml min^{-1}.

4. Conclusions

In this work, on-line, continuous CL detection in GrFFF has been explored with HRP used as a model sample, either free or bound to PS beads. The LoD values for both free and PS-bound HRP were found to be in the femtomole range. On-line, continuous CL detection in GrFFF allows for low-cost and fast determination of the free/bound enzyme mass ratio in mixed samples. The most appealing consequence is then the possibility to realize a flow-assisted immunoassay based on PS bead-immobilized antibodies (PS/Ab) and CL detection. In particular, GrFFF–CL can be applied for competitive immunoassays [27]. Such assays rely on the competition between the analyte (An) present in the sample and an enzyme-labelled analyte derivative (An*) for a limiting amount of immobilized antibody. The key point in the analytical performance of this type of immunoassay is the efficient separation of the labelled analyte in solution from that bound to the specific

antibody, which is therefore itself immobilized on the beads (PS/Ab–An*). The exact evaluation of the amount of PS/Ab–An* is required to get the concentration of An in the sample. This work shows that GrFFF–CL is able to separate and quantify free and bound HRP, which is a necessary condition for the development of competitive immunoassays based on FFF and CL.

FFF-CL-based immunoassays may also offer other advantages with respect to conventional solid-phase methods in microtiter plate format. Firstly, the kinetics of the immunological reaction is likely to be faster, thus reducing analysis time. When nano- or micronsized beads are used as solid phase, the immunological reaction takes place in a dispersed, heterogeneous phase. The solution/solid phase interfacial area is thus much larger than in macro-solid phase immunoassays, in which a layer of Ab is immobilized on the bottom surface of a microtiter plate well. Since the mass transport between the solution and the solid phase surface is likely the rate-limiting step of the immunological reaction, the larger interfacial area of the PS beads gives rise to more favorable kinetics. In addition, FFF-CL-based assays should not require additional washing steps to separate free and bound, labelled analyte as this is performed during the FFF elution. Last but not least, with the size-based separation capabilities of FFF, multianalyte immunoassay methods could be developed. By this way, different immunoassays could be simultaneously performed using beads of different sizes, each coated with a specific antibody, which are fractionated by FFF before CL detection. Moreover, the specificity of FFF-CL immunoassays could rely not only on bead size but also on selective CL detection. For instance, two different analytes, which are captured by the same beads, might be detected separately using bio-specific reagents labelled with different enzymes. The FFF-CL coupling thus retains the advantages of the two analytical techniques, i.e. the high sensitivity, low LoD, and fast kinetics of the CL detection methods, and the powerful size-based fractionation mechanism of FFF. Once feasibility of FFF-CL-based immunoassays has been proven, the system could be miniaturized to reduce reagent costs. Multi-channel configurations should be possible, which could be automated by means of appropriate reagent delivery systems.

Acknowledgements

Work supported by the MIUR (Ministero dell'Istruzione, dell'Università e della Ricerca). The authors wish to thank Ph. Cardot, University of Limoges, for his discussion and suggestions on image analysis of the GrFFF fractionation process.

References

[1] N. Kuroda, M. Kai, K. Nakashima, Chemiluminescence detection in liquid chromatography, in: A.M. Garcia-Campaña, W.R.G. Baeyens (Eds.), Chemiluminescence in Analytical Chemistry, Marcel Dekker, New York, 2001, pp. 393–425.
[2] A.M. Garcia-Campaña, W.R.G. Baeyens, N.A. Guzman, Chemiluminescence detection in capillary electrophoresis, in: A.M. Garcia-Campaña, W.R.G. Baeyens (Eds.), Chemiluminescence in Analytical Chemistry, Marcel Dekker, New York, 2001, pp. 428–472.
[3] A.K. Campbell, Chemiluminescence: Principles and Applications in Biology and Medicine, Ellis Horwood, Chichester, 1988.
[4] M.A. Bacigalupo, A. Ius, P. Simoni, F. Piazza, A. Roda, K.D.R. Setchell, Fresenius J. Anal. Chem. 370 (2001) 82–87.
[5] A. Roda, P. Pasini, M. Guardigli, M. Musiani, M. Mirasoli, Fresenius J. Anal. Chem. 366 (2000) 752–759.
[6] A. Roda, P. Pasini, M. Musiani, S. Girotti, M. Baraldini, G. Carrea, A. Suozzi, Anal. Chem. 68 (1996) 1073–1080.
[7] L.J. Kricka (Ed.), Nonisotopic Probing, Blotting and Sequencing, 2nd ed., Academic Press, San Diego, 1995.
[8] M. Yamaguchi, H. Yoshida, H. Nohta, J. Chromatogr. A 950 (2002) 1–19.
[9] M.E. Schimpf, K.D. Caldwell, J.C. Giddings (Eds.), Field-Flow Fractionation Handbook, Wiley-Interscience, New York, 2000.
[10] P. Reschiglian, A. Zattoni, D. Melucci, G. Torsi, Rev. Anal. Chem. 20 (2001) 239–269.
[11] F. v. d. Kammer, U. Förstner, Water Sci. Technol. 37 (1998) 173.
[12] K. Van Dyke, K. Woodfork, Light probes, in: K. Van Dyke, C. Van Dyke, K. Woodfork (Eds.), Luminescence Biotechnology, CRC Press, Boca Raton, FL, 2001, pp. 3–29.
[13] Ph. Cardot, S. Battu, A. Simon, C. Delage, J. Chromatogr. B 768 (2002) 285–295.

[14] R. Sanz, Ph. Cardot, S. Battu, M.T. Galceran, Anal. 74 (2002) 4496–4504.
[15] R. Chantiwas, J. Jakmunee, R. Beckett, I.D. McKelvie, K. Grudpan, Anal. Sci. 17 (2001) 423–424.
[16] R. Chantiwas, R. Beckett, J. Jakmunee, I.D. McKelvie, K. Grudpan, Talanta, 58 (2002) 1375–1383.
[17] J. Pazourek, J. Chmelik, J. Microcolumn Sep. 9 (1997) 611–617.
[18] P. Reschiglian, D. Melucci, G. Torsi, A. Zattoni, Chromatographia 51 (2000) 87–94.
[19] A. Lucas, F. Lepage, P. Cardot, Cell separations, in: M.E. Schimpf, K.D. Caldwell, J.C. Giddings (Eds.), Field-Flow Fractionation Handbook, Wiley-Interscience, New York, 2000, pp. 471–486.
[20] P. Reschiglian, A. Zattoni, B. Roda, S. Casolari, M.H. Moon, J. Lee, J. Jung, K. Rodmalm, G. Cenacchi, Anal. Chem. 74 (2002) 4895–4904.
[21] L. Pasti, B. Walczak, D.L. Massart, P. Reschiglian, Chemometrics Intell. Lab. Syst. 48 (1999) 21–34.
[22] P. Reschiglian, G. Blo, F. Dondi, Anal. Chem. 63 (1991) 120–130.
[23] F.J. Díaz, K.J. Jr. Balkus, J. Mol. Catal. B: Enzym. 2 (1996) 115–126.
[24] J.M. Davis, in: M.E. Schimpf, K.D. Caldwell, J.C. Giddings (Eds.), Field-Flow Fractionation Handbook, Wiley-Interscience, New York, 2000, pp. 49–70.
[25] A. Roda, P. Pasini, M. Musiani, S. Girotti, M. Baraldini, G. Carrea, A. Suozzi, Anal. Chem. 68 (1996) 1073–1080.
[26] J. Pazourek, J. Chmelik, J. Chromatogr. A 715 (1995) 259–265.
[27] P. Tijssen, Practice and Theory of Enzyme Immunoassays, Elsevier, Amsterdam, 1985.